Critical Speed Variations for Damaged Bridges

Vikram Pakrashi
Assistant Professor, Dynamical Systems and Risk Laboratory, School of Mechanical and Materials Engineering & Marine and Renewable Energy Ireland (MaREI), University College Dublin, Ireland

Alan O'Connor
Professor, School of Civil, Structural and Environmental Engineering, Trinity College Dublin, Ireland

Biswajit Basu
Professor, School of Civil, Structural and Environmental Engineering, Trinity College Dublin, Ireland

ABSTRACT: This paper investigates the variation of critical vehicle speeds arising from damaged beam – moving oscillator interaction, especially in the presence of damage. The traversing speeds of the moving oscillator that result in local maxima of the vertical displacement, the velocity and the acceleration responses of the beam and the oscillator are termed the critical speeds. The variations of critical speeds of a two degree of freedom oscillator are observed for a wide range of damage location and extent for two different types of damage on a simply supported beam. Significant variation of critical speeds is observed due to the presence of damage in the beam. The nature of the variation of the critical speeds is observed to be dependent on the nature of damage. The findings are useful for engineers to identify vehicle speed regions of interest in relation with design, Structural Health Monitoring and response control of bridge-vehicle interaction process.

Keywords: bridge-vehicle interaction, road surface roughness, sampling, structural health monitoring, open crack, damage marker

1. INTRODUCTION

The problem of beam – moving oscillator interaction has been well-researched and is widely used by practicing engineers and researchers to model the interaction of bridges with moving vehicle traversing them. The absolute maximum values of the responses of the bridge and the vehicle expressed as a function of the traversing speed of the vehicle are considered to be a useful set of information obtained from the bridge – vehicle interaction process. A common representation of this information is the dynamic amplification factor (DAF) of the most critical point on the bridge versus the speed of the traversing vehicle. The absolute maximum values of the dynamic displacements and the dynamic stresses over a range of vehicle speeds is obtained as a result and frequency matching can also be isolated by identifying the local maxima values on the DAF versus vehicle speed curve. The global maximum value selected from the multiple local maxima is of special importance within the design speed range of the vehicles concerned since it relates to the absolute maximum values of the dynamic stresses under expected operating conditions of the bridge.

The allowable speeds of vehicles, along with their weight, for bridges have risen significantly over years and there is a trend of opting for high speed trains and vehicle convoys ([1]). As a result, the range of vehicle speeds used in a significant amount of ongoing and existing literature on bridge – vehicle interaction is high ([2]). Although dynamic deflection is a major marker for the bridge – vehicle interaction, additional features like the velocity and the acceleration responses of the bridge and the vehicle have been investigated and related with serviceability aspects like ride comfort ([3]) and

the possible stress increase on vehicle suspension ([4]). Consequently, information on the critical speeds corresponding to the presence of the local maxima of the responses of the bridge and the vehicle over a range of vehicle speeds is deemed valuable. This information is also important from the point of view of a control engineer since passive and semi-active control of bridge – vehicle interaction is an active field ([5], [6], [7], [8]) of research.

Investigations into the nature of the critical speeds are model-based for unsuitability and difficulty of experimental options. Although many two-dimensional ([9], [10], [11]) and three-dimensional models ([12], [13]) exist capturing various local aspects of the bridge – vehicle interaction dynamics, a beam – moving load interaction has often been found to be a good model for describing the global interaction to sufficient accuracy ([14]). In fact, as long as the dynamic deflection of the beam is of concern it is often not even necessary to include the inertial component of the moving force that renders the mass matrix of the combined bridge and vehicle system time dependent. The use of beam – moving oscillator interaction has also been validated successfully in a number of reported experiments ([10],[15]). Literature exists in terms of modelling the bridge – vehicle interaction, reduction of the numerical complexities involved in the modelling and parametric studies ([9]-[14]). Effects of potholes ([16]), surface roughness ([17]) and entry and exit conditions ([18]) have also been looked at in considerable detail.

However, it is important to note that the as-built condition of the bridge can gradually and significantly change over time and may create a shift, drift or variation of the critical speeds associated with the responses of the bridge or the vehicle. Since structural information of a bridge is often not available after it is built, it is important to anticipate the envelope of these shifts or variations of the critical speeds conditions using numerical investigations. The effect of damage depends both on its extent and its position. Such information regarding the variation of critical speed, especially for vehicles can be relevant for drive-by Structural Health Monitoring (SHM) techniques.

This paper presents a numerical study to on the variation of critical speeds related to the vehicle from a damaged beam – quarter car moving oscillator interaction. A simply supported beam with a lumped and a smeared crack has been considered for the studying the effects of varied models of damage. A wide range of damage locations and extents are considered for a range of vehicle speeds and the maximum responses of the displacement, velocity and the acceleration of the moving oscillator are obtained. The critical speeds corresponding to each of the responses are identified for the two different damage models and their distributions for a range of damage locations and extents are investigated.

2. DAMAGE MODEL

Lumped crack and smeared crack models for damage are used in this paper. The lumped crack model is more localized than the smeared crack model and a rotational spring analogy is used to model the lumped crack. This rotational spring analogy is a good substitute to other more detailed and sophisticated continuous crack models. This involves considering a simply supported beam of length L with an open crack located at a distance of ‘a’ from the left hand support of the beam as two uncracked beams connected through a rotational spring at the location of the crack. The crack depth is taken as ‘c’ and the overall depth of the beam is ‘h’. The crack depth ratio (CDR) is defined as c/h and is a measure of the damage extent. The general solution of the modeshape ($\Phi_{(.)}$) from the free vibration equation of the damaged beam can be expressed as

$$\Phi_L = C_{1L}\mathrm{Sin}(\lambda x) + C_{2L}\mathrm{Cos}(\lambda x) + C_{3L}\mathrm{Sinh}(\lambda x) + C_{4L}\mathrm{Cosh}(\lambda x) 0 \le x < a \quad (1.1)$$

and

$$\Phi_R = C_{1R}\mathrm{Sin}(\lambda x) + C_{2R}\mathrm{Cos}(\lambda x) + C_{3R}\mathrm{Sinh}(\lambda x) + C_{4R}\mathrm{Cosh}(\lambda x) a \le x \le L \quad (1.2)$$

for the sub-beams on the left and the right side of the rotational spring respectively. The distance from the left-hand support of the beam is 'x'. The terms $C_{(.)}$ are integration constants arising from the solution of the separated fourth order partial differential equation of free vibration of beam in space. The term λ is expressed as

$$\lambda = \left(\frac{\rho A \omega^2}{EI}\right)^{1/4} \quad (2)$$

where the natural frequency of the cracked beam is ω. The symbols ρ,A, E and I refer to the density of the material of the beam, the cross-sectional area, the Young's modulus of the material of the beam and the area moment of inertia of the beam respectively. Displacements and the moments at the two supports of the beam are zero and continuity in displacement, moment and shear at the location of crack exists. A slope discontinuity is present at the location of the crack location of the crack as

$$\Phi_R'(a) - \Phi_L'(a) = \theta L \Phi_R''(a) \quad (3)$$

where θ is the non-dimensional crack section flexibility dependent on CDR and can be expressed in terms of a polynomial ([19]). The boundary conditions, when substituted in the general modeshape equation, give rise to a set of necessary number of linear equations which can be used to determine the natural frequency of the system by setting the determinant of the linear equation system to zero.

The smeared crack model assumes a reduction of the moment of inertia over an affected width. The damaged beam is analysed as an assembly of three sub-beams, the damaged sub-beam with reduced stiffness positioned in between the two undamaged ones. Continuity in deflection, slope, moment and shear are assumed on both left and right ends of the damaged zone. The modeshape thus consist of twelve coefficients. The coefficients and the natural frequency are found in the same way as of the lumped crack model. A more detailed summary of the models can be found in ([20]).

3. DAMAGED-BEAM AND QUARTER CAR INTERACTION

A simply supported beam with an open crack is traversed at a speed u_0 by a vehicle modelled as a quarter car consisting of two degrees of freedom representing the vertical motions of the wheel and the body respectively. The quarter car comprises of masses corresponding to the lower and the upper degrees of freedom and these are represented as m_w and m_b respectively. A spring – damper assembly consisting of two sets of springs (k_b, k_w) and dampers (c_b, c_w) model the suspension system of vehicle while the angular movements of the vehicle are neglected. Contact loss, bouncing, impact effects and surface roughness are not taken into account to isolate the effects of damage alone. Figure 1 shows the schematic of a damaged beam – moving oscillator interaction.

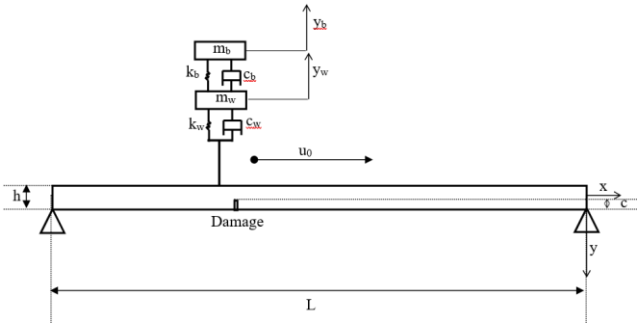

Figure 1. Schematic of Damaged Beam – Moving Oscillator Interaction

Considering the dynamic equilibrium conditions for the degrees of freedom along the displacement directions y_b and y_w (representing the upper and the lower degrees of freedom respectively) the following equations are obtained

$$m_b\ddot{y}_b + c_b(\dot{y}_b - \dot{y}_w) + k_b(y_b - y_w) = 0 \quad (4)$$

$$m_b\ddot{y}_b + m_w\ddot{y}_w + c_w(\dot{y}_w + \dot{y}) + k_w(y_w + y) = 0 \quad (5)$$

where y is the dynamic displacement of the beam. The overdots in equations 1, 2 and 3 are the derivatives with respect to time. The equation for the forced vibration of the beam is

$$EI\frac{\partial^4 y(x,t)}{\partial x^4} + \hat{c}\frac{\partial y(x,t)}{\partial t} + \rho A\frac{\partial^2 y(x,t)}{\partial t^2} = F_P(t) \quad (6)$$

where

$$F_P(t) = (m_b\ddot{y}_b(t) + m_w\ddot{y}_w(t) + (m_b + m_w)g)\,\hat{\delta}(x - u_0t) \quad (7)$$

the acceleration due to gravity being g and $\hat{\delta}$ being the Dirac Delta function. The coefficient of damping of the beam is represented as $\hat{c}$. The dynamic displacement of the beam can be resolved into a number of orthogonal modeshapes using the standard technique of separation of variables. Exploiting the orthogonality of the modeshapes ([21]) a second order differential equation in time is obtained corresponding to each modeshape as

$$\ddot{q}_j(t) + 2\xi_j\omega_j\dot{q}_j(t) + \omega_j^2 q_j(t) = R_j(t) \quad (8)$$

where ω_j denotes the natural frequency and ξ_j denotes the damping ratio of the beam for j^{th} mode. The forcing function $R_j(t)$ is

$$R_j(t) = \frac{1}{\rho A\hat{K}}\{(m_w\ddot{y}_w + m_b\ddot{y}_b + (m_w + m_b)g\}\Phi_j(u_0t)\} \quad (9)$$

where the constant $\hat{K}$ is defined as the integral of the squared modeshape over the length. The acceleration of the vehicle and the effects of damage both enter into the dynamic loading of the beam. The system of dynamic equations can be represented into a matrix form and solved for the responses of the various degrees of freedom. Closed form solutions for the response of the beam can be obtained with sufficient accuracy by considering a simplified beam – moving force interaction model. Consider a simply supported beam with an open crack being traversed simultaneously by n number of concentrated loads P_i (i from 1 to n) moving with a speed u_0. The forced vibration equation is

$$EI\frac{\partial^4 y(x,t)}{\partial x^4} + \hat{c}\frac{\partial y(x,t)}{\partial t} + \rho A\frac{\partial^2 y(x,t)}{\partial t^2} = \sum_{i=1}^{n} P_i\,\hat{\delta}(x - u_0t) \quad (10)$$

The result for the first mode is shown as it contributes more significantly than the higher modes. Solutions involving higher modes are similar. Considering the first mode of the beam, by the method of separation of variables

$$y(x,t) = \Phi(x)q(t) \quad (11)$$

where q(t) is the temporal response of the beam. By substituting equation 11 in equation 10, multiplying both sides by Φ(x), integrating over the length and rearranging, gives

$$\ddot{q}(t) + 2\xi\omega\dot{q}(t) + \omega^2 q(t) = \sum_{i=1}^{n}\frac{P_i}{\rho A\hat{K}}\Phi(u_0t) \quad (12)$$

where

$$\hat{K} = \int_0^L \Phi(x).\Phi(x)dx \quad (13)$$

A term D_{ij} is defined as

$$D_{ij(.)} = \frac{P_i C_{j(.)}}{\rho AK} \quad (14)$$

where $C_{j(.)}$ are coefficients of the modeshapes obtained from the rotational or the smeared crack model. The force of excitation F(t) is

$$F(t) = D_{i1(.)}\mathrm{Sin}\lambda(u_0t) + D_{i2(.)}\mathrm{Cos}\lambda(u_0t) + D_{i3(.)}\mathrm{Sinh}\lambda(u_0t) + D_{i4(.)}\mathrm{Cosh}\lambda(u_0t) \quad (15)$$

where λ is defined as before. Choosing the solution to be

$$q(t) = G_{i1(.)}Sin\lambda(u_0 t) + G_{i2(.)}Cos\lambda(u_0 t) + G_{i3(.)}Sinh\lambda(u_0 t) + G_{i4(.)}Cosh\lambda(u_0 t) \quad (16)$$

and substituting in equation 12, we obtain

$$\begin{bmatrix} \omega^2 - \lambda^2 u_0^2 & -2\xi\omega\lambda u_0 & 0 & 0 \\ 2\xi\omega\lambda u_0 & \omega^2 - \lambda^2 u_0^2 & 0 & 0 \\ 0 & 0 & \omega^2 + \lambda^2 u_0^2 & 2\xi\omega\lambda u_0 \\ 0 & 0 & 2\xi\omega\lambda u_0 & \omega^2 + \lambda^2 u_0^2 \end{bmatrix} \times \begin{Bmatrix} G_{i1(.)} \\ G_{i2(.)} \\ G_{i3(.)} \\ G_{i4(.)} \end{Bmatrix} = \begin{Bmatrix} D_{i1(.)} \\ D_{i2(.)} \\ D_{i3(.)} \\ D_{i4(.)} \end{Bmatrix} \quad (17)$$

The terms $G_{ij(.)}$ are solved as

$$G_{i1(.)} = \frac{(\omega^2 - \lambda^2 u_0^2)D_{i1(.)} + (2\xi\omega\lambda u_0)D_{i2(.)}}{(\omega^2 - \lambda^2 u_0^2)^2 + (2\xi\omega\lambda u_0)^2} \quad (18)$$

$$G_{i2(.)} = \frac{-(2\xi\omega\lambda u_0)D_{i1(.)} + (\omega^2 - \lambda^2 u_0^2)D_{i2(.)}}{(\omega^2 - \lambda^2 u_0^2)^2 + (2\xi\omega\lambda u_0)^2} \quad (19)$$

$$G_{i3(.)} = \frac{(\omega^2 + \lambda^2 u_0^2)D_{i3(.)} - (2\xi\omega\lambda u_0)D_{i4(.)}}{(\omega^2 + \lambda^2 u_0^2)^2 - (2\xi\omega\lambda u_0)^2} \quad (20)$$

$$G_{i4(.)} = \frac{-(2\xi\omega\lambda u_0)D_{i3(.)} + (\omega^2 + \lambda^2 u_0^2)D_{i4(.)}}{(\omega^2 + \lambda^2 u_0^2)^2 - (2\xi\omega\lambda u_0)^2} \quad (21)$$

Such closed form solutions are only for the beam response for special cases and often it is more appropriate to obtain the response of the beam and the quarter car numerically. The inertial component in the forcing term can produce several local maxima in the lower speed regions and it is required to find out how the presence of damage affects the spread if those speeds corresponding to the local maxima. This effect cannot be captured by a closed form response ignoring the inertial effects. Since hyperbolic terms enter into the modeshape equation, it is apparent that the locations of the local maxima can shift in the critical speed versus beam or oscillator response curves. The shift of the critical speeds cannot be ascertained through sensitivity analyses employed by relating small changes in natural frequency due to small changes in damage due to the presence of these new terms.

4. RESULTS

The damaged beam – moving oscillator interaction is simulated up to a velocity range of 300 km/hr with an increment of 0.1 km/hr. Damage conditions in terms of crack depth ratio (0-0.35) and position (fourteen equally spaced locations from the support to midspan) are considered in this regard for both rotational spring and smeared crack models.

Table 1. Values of parameters of beam and moving oscillator.

Oscillator	$\mathbf{m_b}$=5000 kg $\mathbf{m_w}$=35000 kg	$\mathbf{c_b}$=6x10^4 N-s/m $\mathbf{c_w}$=6x10^4 N-s/m	$\mathbf{k_b}$=5.1x10^6 N/m $\mathbf{k_w}$=9.6x10^6 N/m
Beam	**A**=9.22 m^2 **I**=1.5 m^4 **L**=45m	ρ=2x10^3 kg/m^3 **E**=35x10^9 N/m^2	ξ_j = 3%

The details of the values of various parameters involved are provided is Table 1. The width of the smeared crack is assumed to be 1% of the length of the beam. The beam and the two degrees of the freedom of the oscillator are assumed have zero initial conditions.

The normalized responses for the lower degree of freedom of the oscillator are presented in Figure 2 where the amplification of the responses is comparatively more pronounced than those for the beam and a range of variation exists. The nature of the responses of the beam and the oscillator is dependent on the type of damage present in the beam.

Figure 3 presents the histograms of the variation of the critical speeds associated with the vertical displacement, velocity and acceleration responses of the beam and the two degrees of freedom of the moving oscillator for a rotational spring model considering the entire damage range.

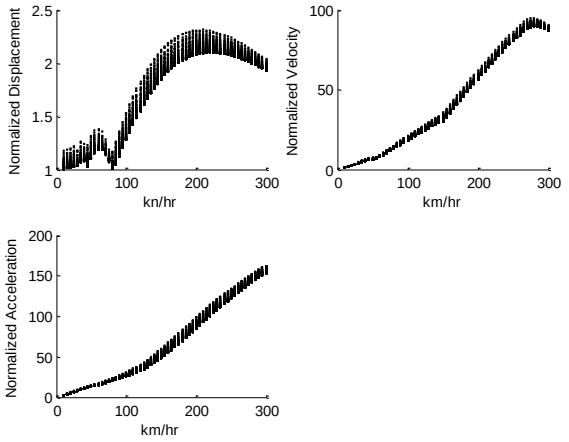

Figure 2. Normalized Responses of Lower Mass of the Moving Oscillator for a Range of Damage Conditions (Rotational Spring Model) versus the Speed of the Traversing Oscillator

Figure 4 presents the same histograms as has been presented in Figure 3, but for a smeared crack model of damage. The significant variation of critical speeds for both cases is apparent.

The lower speed range of the oscillator is observed to be generating a nearly continuous region of interest due to the formation of closely spaced maxima values. The generation of closely spaced maxima values is chiefly due to the inertial component of the oscillator excitation. Thus, for lower speed regions of the traversing oscillator, the definition of critical speed corresponding to maxima values of bridge or oscillator responses is not helpful. For such range of traversing speeds, it is more important to set a preselected limiting value for the response and then consider the traversing speed range of the oscillator corresponding to all responses exceeding that preselected response value to be of region of interest. The choice of the model does not significantly affect the region of interest under these circumstances. The low traversing speed region must be interpreted as a relative value with respect to the speed corresponding to the global maximum of the responses. The critical speed range corresponding to the absolute global maximum responses is clustered separate from those corresponding to low traversing speeds of the oscillator.

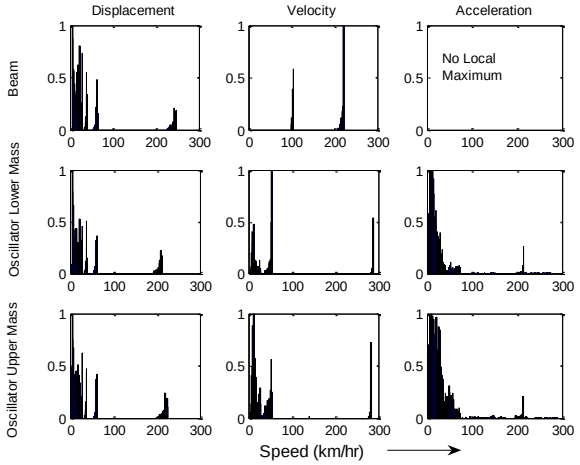

Figure 3. Histogram of Variation of Critical Speeds for Smeared Crack Model

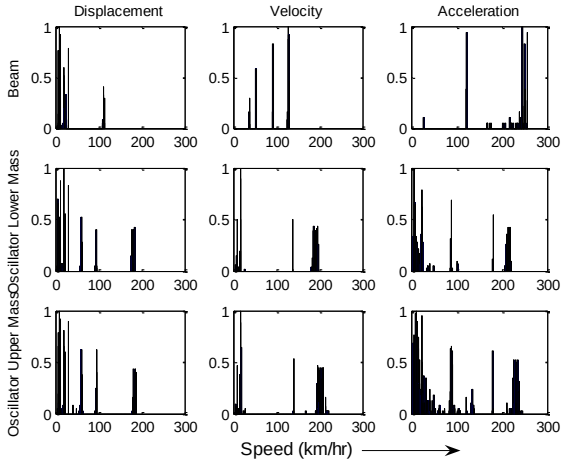

Figure 4. Histogram of Variation of Critical Speeds for Rotational Spring Model

They are observed to be varying significantly. As a result, the speeds that produce the absolute maximum dynamic stresses vary significantly. These clusters are narrow and well defined. Consequently, the definition of critical speeds related with the identification of a maximum of the response is valid. The clusters of critical speed zones are observed to have been formed for different responses and damage models. The location of these clusters shift according to the

type of response and the damage models. When no information is available regarding the anticipated type of damage, a pooled set of simulations can be used. Under these circumstances relatively narrower bands (with respect to the continuous band in the low traversing speed range) of critical velocities are formed with well-defined clustering. The choice for a vibration control system for the suppression of the global response would then be directed towards suppressing those clustered critical speed ranges. Since the spread of the critical speeds are significant potential robust control systems should cater for the anticipated spread. When information regarding the anticipated type of damage is known or agreed upon, certain damage mechanisms or models, and subsequently certain clusters of interest can be ignored. Figures 3 and 4 are thus observed to be useful as a guideline of velocity regions of interest based on the degree of freedom, the type of region and the type of damage considered. The figures also illustrate the importance of the variable definition of critical speeds in the high and low speed regions of the traversing oscillator.

5. CONCLUSIONS

The variation of critical vehicle speeds for a damaged beam – moving oscillator interaction is studied in this paper. It is observed, that damage introduces variation of critical speeds. The critical speeds corresponding to the absolute global maxima of responses form well defined clusters of their own in the high traversing speed range and undergo significant variation due to the presence of damage. The histograms of critical speed variation indicate that the nature and the extent of the variations over a given domain of vehicle speeds are dependent on the nature of damage present in the beam. In the low traversing speed region, a wide range of speeds correspond to local maxima values of responses due to inertial effects of the moving oscillator. Under such conditions, the definition of critical speed, or the critical speed region of interest should not be related to the formation of a local maximum of a response. Rather, the exceedence of a preselected value of a response for a traversing speed range should be considered as critical. This duality of definition is important since many bridge structures are traversed by vehicles below a certain maximum allowable speed. The findings are potentially useful in terms of identifying anticipated velocity regions of interest for a bridge – vehicle interaction problem where information of the as built condition of the bridge over a long time is usually limited. It is also valuable in terms of identifying potential velocity bands for vibration suppression and the choice of control methods to reduce the responses of the bridge or the vehicle.

ACKNOWLEDGEMENTS

The first author acknowledges Science Foundation Ireland Centre Marine and Renewable Energy Ireland (MaREI) centre funding 12/RC/2302.

REFERENCES

[1] Li J, Su M. The Resonant Vibration for a Simply Supported Girder Bridge Under High Speed Trains. Journal of Sound and Vibration 1999; 224(5): 897-915.

[2] Xia H, Zhang N, Guo WW. Analysis of Resonance Mechanism and Conditions of Train – Bridge System. Journal of Sound and Vibration 2006; 297: 810-22.

[3] Wu YS, Yang YB. Steady – State Response and Riding Comfort of Trains Moving Over a Series of Simply Supported Bridges. Engineering Structures 2003; 25: 251-65.

[4] DeBrunner V ,Ta M. On the Design of Structural Vibration Control Systems for Highway Bridges. IEEE Intelligent Vehicles Symposium, Parma, Italy 2004.

[5] Kwon HC, Kim MC, Lee IW. Vibration Control of Bridges Under Moving Loads. Computers & Structures 1998; 66(4): 473-480.

[6] Patten WN, Sack RL, He Q. Controlled Semiactive Hydraulic Vibration Absorber for Bridges. Journal of Structural Engineering ASCE 1996; 122(2): 187 – 92.

[7] Li J, Su M, Fan L. Vibration Control of Railway Bridges under High – Speed Trains using Multiple Tuned Mass Dampers. Journal of Bridge Engineering ASCE 2005; 10(3): 312-20.
[8] Ahmadian M, Pare CA. A Quarter – Car Experimental Analysis of Alternative Semiactive Control Methods. Journal of Intelligent Material Systems and Structures 2000; 11:604 – 12.
[9] Xia H, Zhang N, De Roeck G. Dynamic Analysis of High – Speed Railway Bridge under Articulated Trains. Computers & Structures 2003; 81: 2467 – 78.
[10] Green MF, Cebon D. Dynamic Response of Highway Bridges to Heavy Vehicle Loads: Theory and Experimental Validation. Journal of Sound and Vibration 1994; 170(1): 51 – 78.
[11] Zhu XQ, Law SS. Dynamic Load on Continuous Multi – Lane Bridge Deck from Moving Vehicles. Journal of Sound and Vibration 2002; 251(4): 697 – 716.
[12] Song MK, Noh HC, Choi CK. A new three-dimensional finite element analysis model of high-speed train–bridge interactions. Engineering Structures 2003; 25(13), 1611-1626.
[13] Wu YS, Yang YB, Yau JD. Three – Dimensional Analysis of Train – Rail – Bridge Interaction Problems. Vehicle System Dynamics 2001; 36(1): 1 – 35.
[14] Bilello C, Bergman LA, Kuchma D. Experimental Investigation of a Small – Scale Bridge Model under a Moving Mass. Journal of Structural Engineering ASCE 2004; 130(5): 799 – 804.
[15] Fryba L. Dynamics of Railway Bridges. Thomas Telford, London 1996.
[16] Pesterev AV, Bergman LA, Tan CA, Yang B. Assessing Tire Forces Due to Roadway Unevenness by the Pothole Dynamic Amplification Factor Method. Journal of Sound and Vibration 2005; 279: 817 – 41.
[17] Li Y, OBrien E, Gonzalez A. The Development of a Dynamic Amplification Estimator for Bridges with Good Road Profiles. Journal of Sound and Vibration 2006; 293: 125 – 37.
[18] Shi X, Cai CS, Chen S. Vehicle Induced Dynamic Behaviour of Short Span Slab Bridges Considering Effect of Approach Slab Condition. Journal of Bridge Engineering ASCE 2008; 13(1): 83 – 92.
[19] Narkis Y. Identification of Crack Location in Vibrating Simply Supported Beams. Journal of Sound and Vibration 1994; 172(4): 549-558.
[20] Pakrashi V, Basu B, O' Connor A. Structural Damage Detection and Calibration using Wavelet-Kurtosis Technique. Engineering Structures 2007; 29: 2097 – 2108.
[21] Jo BW, Tae GH, Lee DW. Structural Vibration of Tuned Mass Damper Installed Three Span Steel Box Bridge. International Journal of Pressure Vessels and Piping 2001; 78: 667-675.